Suppressing Delay-Induced Oscillations in Physical Human-Robot Interaction with an Upper-Limb Exoskeleton using Rate-Limiting

Jianwei Sun[1], Peter Walker Ferguson[1], and Jacob Rosen[1]

***Abstract*— In physical human-robot interaction (pHRI) enabled by admittance control, delay-induced oscillations arising from both the neuromuscular time-delays of the human and electromechanical delays of the robot can cause unsafe instability in the system. This study presents and evaluates rate-limiting as a means to overcome such instability, and provides a new perspective on how rate-limiting can benefit pHRI. Specifically, a rate-limited and time-delayed human-in-the-loop (HITL) model is analyzed to show not only how the rate-limiter can transform an unstable equilibrium (due to time-delay) into a stable limit-cycle, but also how a desired upper-bound on the range of persistent oscillations can be achieved by appropriately setting the rate-limiter threshold. In addition, a study involving 10 subjects and the EXO-UL8 upper-limb exoskeleton, and consisting of 16 trials - 4 rate-limiter thresholds by 4 time-delays - is performed to: (1) validate the relationships between time-delays, rate-limits, and position bounds on persistent oscillations, and (2) demonstrate the effectiveness of rate-limiting for recovery from delay-induced oscillations without interfering with regular operation. Agreement of experimental results with the theoretical developments supports the feasibility of incorporating rate-limiting in admittance-controlled pHRI systems as a safety mechanism.**

***Index Terms*— Physical human-robot interaction (pHRI), upper-limb exoskeleton, rehabilitation robots, human-in-the-loop, admittance control, safety, rate-limiting.**

I. Introduction

Physical human-robot interaction (pHRI) is a necessary component of any exoskeleton-assisted physical therapy. Often enabled through admittance control, such pHRI allows the exoskeleton to fluidly follow the motions of the human operator. This functionality allows the exoskeleton to precisely apply assistive forces to the operator in order to create an effective training environment. Naturally, safety is a primary concern when interacting with powered robotic devices, as the target audience of such physical therapy often has limited physical capability.

Even though the exoskeleton's admittance controller renders it a stable system by itself, the feedback connection of the human with the exoskeleton, along with neuromuscular delays of the human and electromechanical delays of the robot, can cause dangerous unstable oscillations. As discussed in [1], a human's natural tendency is to stiffen in order to suppress oscillations, but this can actually increase instability. An intuitive response to handling the instability is to add low-pass filtering, which assumes that removing high frequency components can bound velocity. However, not only is this false, low-pass filtering also introduces $-(\pi/2)n$ radians of phase lag for high-frequency components, where n is the filter's order. This phase lag reduces the system's phase margin and responsiveness to the operator, and can even be destabilizing [1]. Thus, ensuring stability in these *human-in-the-loop* (HITL) systems is non-intuitive, and must be addressed from the exoskeleton's point of view.

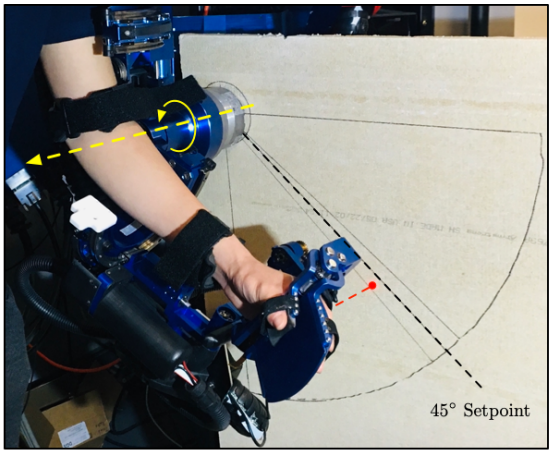

(a) Experiment Setup

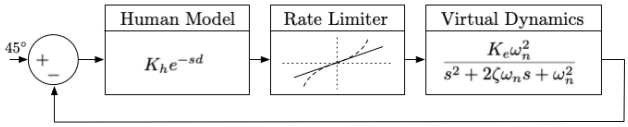

(b) Human-in-the-Loop Model

Fig. 1. (a) Experiment setup using the left elbow of the EXO-UL8 upper-limb exoskeleton. Subjects must track the 45° setpoint for various values of time-delay and rate-limiter thresholds. A laser pointer (enhanced in red) provides visual feedback to the subjects. (b) A block diagram of the HITL used in the theoretical developments of sections II and III.

Various studies have proposed different methods of ensuring safety in pHRI, including, but not limited to: ensuring passivity of the system [2], [3], [4], [5], [6], reducing phase-lag through feedforward control [7], [8], [9], saturating forces/torques [10], [11], using adaptive control to ensure robustness against modeling uncertainties [12], and dynamically adjusting admittance control parameters [13], [14], [15], [16], [17].

Motivated by nonlinear control theory, passivity-based controllers ensure stability by preventing the feedback system from accumulating unbounded energy. Previous literature shows the utility of passivity-based approaches, such as in designing stabilizing controllers for exoskeletons [2], [4], mitigating communication delays in teleoperation [3], and overcoming modeling uncertainties [5]. While passivity-

[1]The authors are with Department of Mechanical and Aeropsace Engineering at the University of California, Los Angeles (UCLA), USA 90095. {sunjianwl, pwferguson, jacobrosen}@ucla.edu

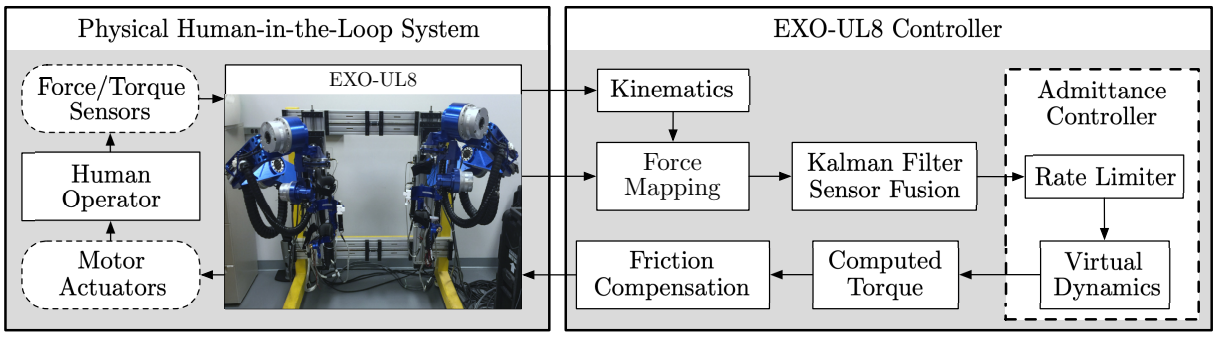

Fig. 2. Block diagram of the EXO-UL8's control architecture with the admittance controller shown in the dash-outlined box on the right. The rate-limiter outputs the filtered estimated human-applied torques, which propagate the virtual dynamics. The trajectories of the virtual dynamics are then tracked by the computed torque controller, which also compensates for gravity and link inertia. On the physical side, the operator interacts with the EXO-UL8 through force/torque sensors and motor actuators, which are shown in the dashed round blocks but are considered as part of the EXO-UL8.

based control is effective for ensuring stability, the controller requires knowledge of the passivity properties of the human, which may be difficult to precisely determine.

Another technique for improving stability is to reduce phase-lag in the HITL system by utilizing disturbance observers to provide feedforward compensation [7], [8], [9]. For these systems, the controller requires measuring or estimating the robot's acceleration, which can be susceptible to modelling errors. A simpler method is to just saturate the human-applied forces by limiting the maximum values measured. While this can prevent divergence in some cases, it is inadequate in general because: (1) it is unclear how the saturation threshold should be set to prevent instability without interfering with regular high-speed interaction, (2) saturation does not prevent high frequency switching between threshold values, and (3) it may result in the "wall-sticking" problem described in [6] which can produce undesirable performance.

Safety has also been addressed by detecting instability using various heuristics and then dynamically adjusting the admittance control parameters [13], [14], [15], but this requires tuning based on experimental data and may not generalize to other HITL robotic systems.

In this paper, we present a new perspective on rate-limiting as a safety mechanism against delay-induced instability. Rate-limiting is traditionally regarded as an undesirable nonlinearity since it is difficult to compensate for, as seen in early fighter jets [18], [19]. Subsequent studies have therefore investigated various other methods for prediction and compensation [20], [21], [22]. However, rate-limiting has useful properties that can benefit pHRI. In this work, we propose and experimentally validate the incorporation of a rate-limiting filter to our admittance controller to prevent delay-induced instability for the EXO-UL8 upper-limb exoskeleton. Even though the filter does not guarantee equilibrium stability, it prevents trajectories from diverging and can allow the human operator to recover from unstable oscillations. We believe that the rate-limiting filter can improve safety in admittance control-based pHRI because it does not require precise dynamical/passivity models of the human, does not require estimating acceleration, can overcome issues with high frequency switching apparent in force/torque saturation methods, avoids the need for any detection of instability, and is simple to implement. Our contributions are therefore:

1) Theoretically analyzing the rate-limiter in a HITL system, as shown in Fig. 1, and demonstrating how persistent oscillations due to large time-delays can be bounded as desired by selection of rate-limiter threshold,
2) Validating the rate-limiter on an upper-limb exoskeleton for 10 subjects to empirically demonstrate utility,
3) Demonstrating the effect of time-delay for the HITL system and how rate-limiting can prevent instability to allow for recovery from persistent oscillations.

II. Model of Human-in-the-Loop

The EXO-UL8 is a bimanual upper-limb exoskeleton comprised of a pair of serial manipulator arms, each with 7 active *degrees-of-freedom* (DoFs), developed to support research in pHRI and stroke rehabilitation. Admittance control is utilized to enable physical interaction by sensing human input using force/torque sensors located along the exoskeleton's arm and then converting it into equivalent torques at the exoskeleton's joints. These torques then drive virtual dynamic models consisting of decoupled second-order systems with low virtual masses, whose dynamics are then tracked by the exoskeleton's computed-torque controller, as shown in Fig. 2. The overall effect is that to the human, the exoskeleton appears to move according to the virtual dynamics. More information about the sensing and control architecture of the EXO-UL8 can be found in [23], [24].

Consider the simplified HITL model consisting of a single second-order *linear time-invariant* (LTI) system (to represent a single DoF of the exoskeleton's virtual dynamics) in feedback with a static gain, as shown in Fig. 1. By design, the exoskeleton system is stable as its poles are located in the *open left half-plane* (OLHP) at $\{-\sigma \pm j\omega_d\}$, where $\sigma = \zeta\omega_n$, $\omega_d = \omega_n\sqrt{1-\zeta^2}$, ω_n and ω_d are the natural and damped frequencies of the virtual second-order dynamics, respectively, and ζ is the damping ratio. The human interaction is modeled as a static gain, similar to [19], with delay. The static gain represents human-applied forces trying to drive the exoskeleton to a constant setpoint (taken as zero without loss of generality by using error coordinates), while the delay models neuromuscular delay [25].

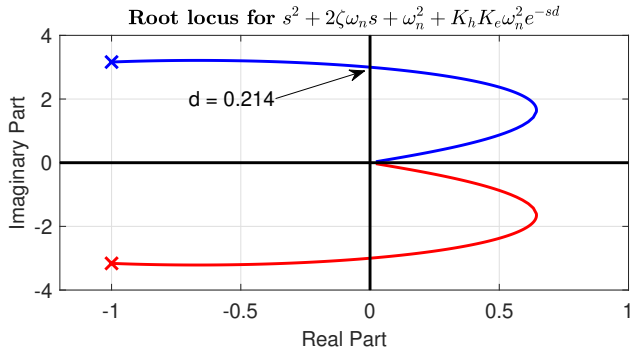

Fig. 3. A root locus for the closed-loop system shows that the closed-loop poles cross the imaginary axis for a sufficiently large time-delay.

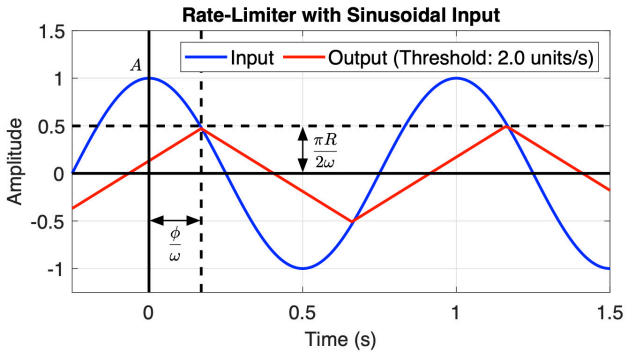

Fig. 4. A sinusoidal input with amplitude greater than or equal to $\frac{\pi R}{2\omega}$ results in a triangular waveform output. In this example, the rate-limiter threshold is set to $R = 2$, and the input has amplitude $A = 1$ and frequency $\omega = 2\pi$. By inspection, the fundamental harmonic of the output is phase-lagged and has decreased amplitude. Furthermore, the triangular waveform has frequency components at multiples of the fundamental harmonics not present in the input signal, which is characteristic of the filter's nonlinearity.

A. Instability due to Time-Delays

Even though both the human and the exoskeleton are stable systems individually, their feedback connection is not necessarily stable. This is shown by considering the stability of the closed-loop system as a function of the time-delay, $d \in \mathbb{R}_{\geq 0}$. As the closed-loop system is still LTI, stability can be assessed by its characteristic polynominal:

$$s^2 + 2\zeta\omega_n s + \omega_n^2 + K_h K_e \omega_n^2 e^{-sd}. \tag{1}$$

A root-locus of the zeros of the characteristic polynominal is shown in Fig. 3 with sample values: $K_h = 10$, $K_e = 1$, $\zeta = 1$, $\omega_n = 1$. The branches cross the imaginary axis, indicating that a sufficiently large time-delay can destabilize the system.

III. Rate-Limiting Filter

Consider the rate-limiting filter added after the human input in Fig. 1. Also known as slew rate-limiting, the nonlinear filter places bounds on the maximum and minimum rates of change of the input signal. In continuous time, the rate-limiter can be implemented as a first-order filter with saturation:

$$\dot{y}(t) = \mathrm{sat}_R(pu(t) - py(t)), \tag{2}$$

where $R > 0$ is the rate-limiter threshold, $u(t)$ is the input scalar signal, $y(t)$ is the output scalar signal, and $p > 0$ is a constant chosen to be much larger than the other system poles. The saturation function is defined as:

$$\mathrm{sat}_R(x) := \begin{cases} -R, & \text{if } x \leq -R, \\ x, & \text{if } -R < x < R, \\ R, & \text{if } R \leq x. \end{cases} \tag{3}$$

A. HITL System with Rate-Limiting

The rate-limiter is added to the HITL system as shown in Fig. 1 to limit the maximum rate-of-change of the human-applied torque. The rate-limiter's output depends on the input signal's frequency and amplitude, and also introduces additional frequency components not present in the input signal. To analyze the effect of the rate-limiter on the HITL system, it is useful to first determine the phase lag of the filter, which helps in calculating the period of the limit cycle in the closed-loop system.

1) Phase Lag of Rate-Limiter: Consider a sinusoidal signal of amplitude A and angular frequency ω input to the rate-limiter with rate-limiter threshold R such that:

$$A \geq \frac{\pi R}{2\omega}, \tag{4}$$

which ensures that the rate-limit is always active, as shown in Fig. 4. The output signal is a periodic triangular wave whose fundamental has the same frequency as the input, but with reduced amplitude and additional phase lag. The phase lag, ϕ, of the output's fundamental harmonic can be determined by considering the start time as the crest of the input and noting that the maximum value of the output is $\frac{\pi R}{2\omega}$. Then, the phase can be calculated by solving for ϕ in:

$$A\cos(\phi) = \frac{\pi R}{2\omega}, \tag{5}$$

to yield:

$$\phi = \cos^{-1}\left(\frac{\pi R}{2A\omega}\right), \tag{6}$$

which is a function of both input frequency and amplitude. Also unlike that of high-order linear filters, the phase lag of the rate-limiter is upper-bounded by $\pi/2$, occurring when inputs have high frequency and high amplitude. This difference demonstrates one intuitive reason for how a rate-limiter can prevent instability in the closed-loop system.

2) Limit Cycle Frequency and Bound on Position: The objective now is to compute the resonant frequency, ω, of the HITL system. To do this, first consider the LTI virtual dynamics of the exoskeleton system. Its phase lag is a function of the input signal's frequency, so the response of the system to a triangular wave input oscillating at ω can be computed. For an even periodic triangular waveform with frequency ω (and consequently, period $T = \frac{2\pi}{\omega}$) defined as:

$$x_T(t) := \begin{cases} \frac{RT}{4} - Rt, & \text{if } t \in \left[0, \frac{T}{2}\right), \\ -\frac{3RT}{4} + Rt, & \text{if } t \in \left[\frac{T}{2}, T\right), \end{cases} \tag{7}$$

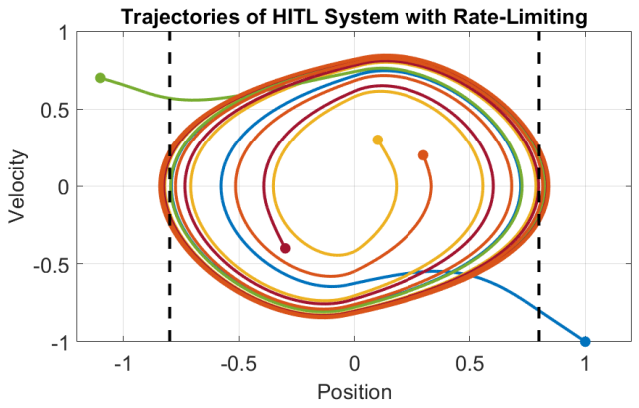

Fig. 5. Trajectories of the HITL with rate-limiter threshold set according to equation (14) for $\epsilon = 0.8$ (shown as dashed lines). Since the closed-loop system is a delayed differential equation, trajectories can cross each other because the system's instantaneous state does not uniquely determine its derivative. Certain trajectories appear to exceed the desired ϵ boundary due to the decaying contributions of the initial conditions; ϵ is a bound on the steady-state oscillations. For all trajectories starting close to the limit cycle, their steady-state behavior approaches the stable limit cycle.

it can be expressed as a sum of its harmonics:

$$x_T(t) = \sum_{n=-\infty}^{\infty} \left(\frac{\pi R}{2\omega}\right) c_n e^{jn\omega t}, \tag{8}$$

$$c_n = \frac{4\sin\left(\frac{\pi n}{2}\right)^2}{\pi^2 n^2}. \tag{9}$$

Let the Fourier transform of the second-order exoskeleton system be denoted as $G(\cdot) : \mathbb{C} \to \mathbb{C}$. Since it is LTI, its output for the input signal x_T is a superposition of the input's harmonics:

$$y_T(t) = \sum_{n=-\infty}^{\infty} \left(\frac{\pi R}{2\omega}\right) c_n \left|G(j(nw))\right| e^{j[n\omega t + \angle G(jnw)]}. \tag{10}$$

Since the phase lag of the rate-limiter also depends on its input signal's amplitude, it is helpful to compute the ratio of the input and output signal maximum amplitudes for G. The amplitude of the input triangular wave is $\frac{\pi R}{2\omega}$, but the output signal attains its maximum value at the delay corresponding to the phase lag of the fundamental harmonic, which is $-\angle G(j\omega)$. Hence, the ratio of input and output maximum amplitudes as a function of frequency, denoted by the function $r(\cdot) : \mathbb{R} \to \mathbb{R}$, can be calculated as:

$$r(\omega) := \sum_{n=-\infty}^{\infty} c_n \left|G(j(nw))\right| e^{j[\angle G(jnw)) - \angle G(j\omega)]}, \tag{11}$$

which does not depend on the rate-limiter threshold, R. Next, to compute the resonant frequency, ω, of the HITL closed-loop system as shown in Fig. 1, consider the gain around the loop. If the rate-limiter's output amplitude is $\frac{\pi R}{2\omega}$, then this amplitude becomes

$$A = K_h r(\omega) \frac{\pi R}{2\omega}, \tag{12}$$

as the signal makes its way around the loop to the rate-limiter's input. When $K_h r(\omega) \geq 1$, the condition in equation (4) is satisfied, and the rate-limiter is always active. For persistent oscillations to occur, the phase lags contributed by the rate-limiter, time-delay, and the exoskeleton system also must result in one period of oscillation. This is described by:

$$\angle G(j\omega) - \cos^{-1}\left(\frac{1}{K_h r(\omega)}\right) - \omega d - \pi = -2\pi, \tag{13}$$

where the first term is the phase lag of the exoskeleton system, the second is from the phase lag of the rate-limiter by substituting equation (12) into equation (6), the third is from the time-delay, and $-\pi$ is from the negative input to the summation block. As an example, solving equation (13) numerically with the same parameters as in Fig. 3 and $d = 0.3$ s yields an oscillation frequency of $\omega = 0.955$ rads/s.

Once ω is determined, the output position can then be bounded to $\pm\epsilon$ by selecting a rate-limiter threshold of:

$$R \leq \frac{2\omega\epsilon}{\pi r(\omega)}. \tag{14}$$

Thus, the size of the stable oscillation can be set as desired for the given virtual dynamics of the system. Fig. 5 shows the stable limit cycle with the desired bounds. This analysis shows the feasibility of rate-limiting as a safety mechanism for human-exoskeleton interaction as unstable trajectories no longer diverge due to time-delay instability, but rather flow in a limit cycle, allowing the human to recover.

IV. Implementation

The EXO-UL8's admittance controller consists of decoupled virtual dynamics at each revolute joint, and converts human-applied forces (inputs) into reference trajectories (output). Rate-limiters are placed between the human-applied forces and the virtual dynamics as shown in Fig. 2. A discrete-time implementation of the rate-limiter dynamics from equation (2) is given in equation (15), which uses the saturation function in equation (3). In the equation, u_k and y_k are the filter's input and output, respectively; Δt is the period of the software loop, and R is the rate-limiter threshold:

$$y_k = y_{k-1} + \text{sat}_{(\Delta t)R}(u_k - y_{k-1}). \tag{15}$$

V. Experiments

A. Experiment Setup

A series of setpoint tracking experiments are performed to validate the expected relationships between time-delay, rate-limiter threshold, and the bound on position for persistent oscillations. The experiment consists of 16 trials: 4 values of rate-limiter threshold for each of 4 values of artificially added time-delay. The experiments are performed on the left elbow flexion DoF of the EXO-UL8, as shown in Fig. 1. In each trial, the subject tries to maintain a constant elbow angle after the experimenter programmatically sends a fixed-magnitude impulse disturbance with random direction. The trial is concluded and marked as unstable if the interaction diverges due to instability. Otherwise, the subject holds the reference position for 15 seconds, as paced by a metronome. An overview of the experimental procedure is presented in

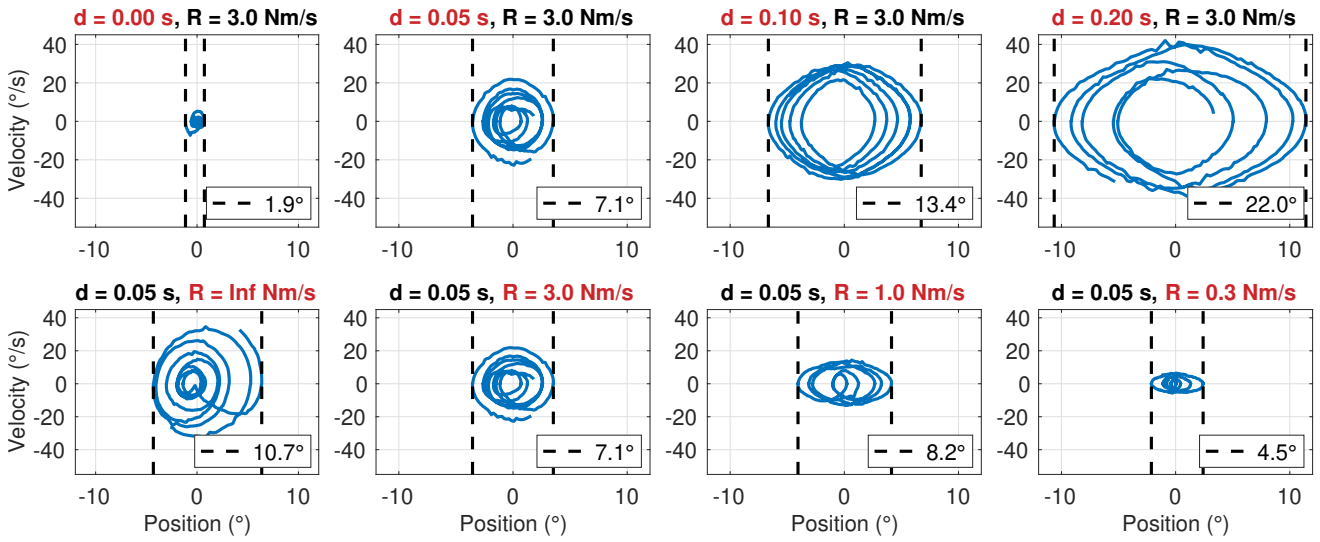

Fig. 6. Zero-mean position and velocity trajectories of subject 1. The top row shows trajectories of persistent oscillations with increasing position range (range shown in the legends) as the time-delay value is increased (highlighted in red) for a constant rate-limiter threshold. The bounds increase monotonically with time-delay. The bottom row shows the effect of decreasing rate-limiter threshold for a fixed time-delay. In this case, the delay is mild and does not result in instability when the rate-limiter is not present (leftmost subfigure). As the threshold decreases, so does the position bound. However, the decrease is not always monotonic, as shown by $R = 1.0$ Nm/s. Simplifying assumptions, such as the human being modeled as a static gain with delay, may be inadequate in capturing complex time-varying behaviors that affect how the human responds to low rate-limiter thresholds.

Procedure 1. A total of 10 subjects (ages: 27.5 ± 2.6; 2 female, 8 male) participated in the study. The experiment is performed in accordance with IRB #18-00766.

B. Results and Discussion

The experiment aims to validate the rate-limiter on the EXO-UL8, and demonstrate that position ranges of persistent oscillations increase with higher time-delays, but decrease with lower rate-limiter thresholds. Experimental trajectories for a sample subject are plotted in Fig. 6. In this figure, increasing time-delay for a fixed rate-limiter threshold results in larger oscillations in steady-state. In contrast, decreasing rate-limiter threshold for a fixed time-delay yields smaller oscillations, suggesting that a lower threshold is needed if the HITL system has significant delay. For this subject, the position bound is slightly larger for $R = 1.0$ Nm/s than for $R = 3.0$ Nm/s; however, this discrepancy can be explained by inter-trial variability of the subject and limitations of the constant gain human model used in the theoretical development. To better evaluate the overall trends, consider the results averaged across all subjects in Fig. 7.

Subject averaged results show that in order to mitigate the enlarging effects of time-delay on steady-state oscillations, the rate-limiter threshold should be reduced. It should also be noted that instability only occurred in trials in which the rate-limiter was inactive ($R = \infty$) and the delay was large ($d \geq 0.1$ s). This suggests that rate-limiting, even with a large threshold, can prevent instability, which was theoretically predicted by the existence of stable limit-cycles in the simulated trajectories of Fig. 5. Furthermore, the undelayed ($d = 0$ s) trials corresponding to $R = 3.0$ Nm/s and $R = \infty$ showed similar position ranges, indicating that the rate-limiter did not significantly affect normal operation.

Procedure 1 Experimental Procedure

for each subject $s \in \{1, \ldots, 10\}$ **do**
  Subject familiarizes with EXO-UL8 for 5 minutes
  for each delay $d \in \{0, 0.05, 0.1, 0.2\}$ **do**
    for each threshold $R \in \{\infty, 3, 1, 0.3\}$ **do**
      Set d and R on EXO-UL8
      Subject moves to $45°$ position
      Experimenter sends $\pm$ impulse disturbance
      if tracking becomes unstable **then**
        Conclude trial
      else
        Subject moves to $45°$ position
        Subject holds for 15 seconds
  Subject reports on experience

This is also supported by the percentage of time that the rate-limiter was active, as shown in Fig. 8. As delays become larger, so do the active times of the rate-limiter in order to overcome the increased likelihood of instability. However, during the undelayed trials, the rate-limiter is still partially active. This is likely a consequence of numerically differentiating the noisy human-applied torque signals, whose derivatives frequently contain impulses exceeding the rate-limiter threshold. By comparing the three different rate-limiter thresholds, it is apparent that while a lower threshold value results in lower amplitude oscillations, as was seen in Fig. 7, too low a value may hinder regular operation.

1) Minimum Rate-Limiter Threshold: For a very small rate-limiter threshold ($R = 0.3$ Nm/s), the position range did not strictly increase with time-delay. Although equation (14) suggests that an arbitrarily small bound can be achieved by a

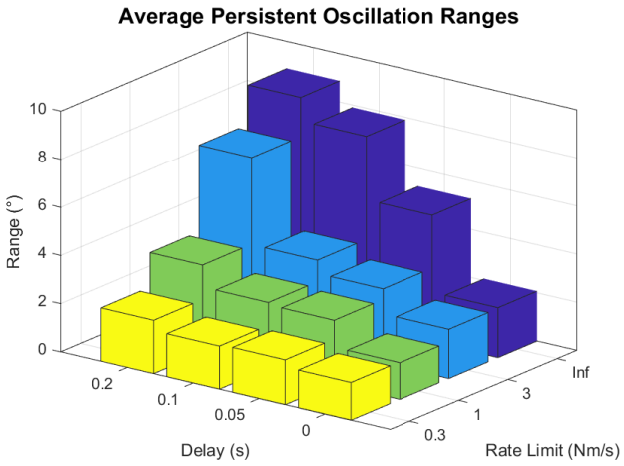

Fig. 7. Position ranges corresponding to 5.5 s of steady-state oscillations of all trials averaged across all subjects. Trials in which subjects experienced instability are recorded as the range exceeding 30°; these only occurred in the absence of the rate-limiter and with delay ≥ 0.1 s.

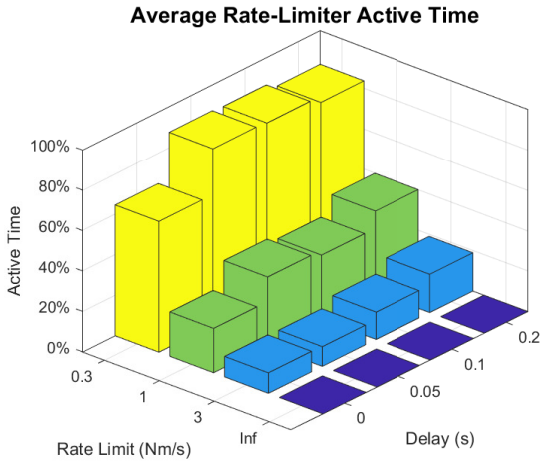

Fig. 8. Active time of the rate-limiter for all trials averaged across all subjects. Greater time delays trigger the rate-limiter more frequently in order to prevent instability. However, longer active times in undelayed trials indicate that too low a threshold may inhibit normal operation.

sufficiently small threshold, the experimental results suggest a minimum threshold beyond which the relationship is no longer valid. The theoretical result assumed that the human can be modeled as a static gain controller with constant delay. While this assumption is sufficient in some cases, these experimental results show the extent to which that assumption is valid. For such a small rate-limiter threshold, the phase delay of equation (13) approaches its maximum, and makes the exoskeleton's motions feel sluggish, as described by subjects in the post-experiment discussions. This is also indicated by the rate-limiter being active 65% of the time at this threshold, even with no added time-delay, as shown in Fig. 8. The increased activity of the rate-limiter and its phase-lag affect the subjects' ability to track the setpoint and cause them to feel less in-control of the exoskeleton, which is a phenomenon not reported for trials corresponding to the larger rate-limiter thresholds. The qualitative and subjective results of the experiments suggest that although rate-limiting is beneficial for mitigating instability, there is a minimum threshold beyond which its limitations outweigh its benefits.

2) Generalization of Rate-Limiter Thresholds: The relationship between the rate-limiter threshold and the oscillation range depends on the virtual dynamics and associated delays of the admittance control system, which do not change across trials and operators; and the electromechanical delays of the operator, which are comparable across individuals [26]. Thus, specific threshold values need only be tuned for each pHRI devices by using a reasonable upper-bound for the operator's delay for the target motion.

3) Recovering from Instability: In a regular HITL system, the rate-limiter is not expected to always be active. Instead, its role is to act as a safeguard by preventing delay-induced oscillations from diverging, while minimizing interference with normal operation. An example of this behavior can be seen in Fig. 9. In this trial, the time-delay is large ($d = 0.2$ s) and destabilization occurs at the 14 s mark, but the rate-limiter prevents the oscillations from diverging. At 20 s, the subject stabilizes and is able to continue normal operation afterward. Causes of instability can include any combination of: the subject becoming fatigued; the subject tensing their arm in an attempt to fight instability [1]; or the subject losing concentration and relying purely on haptic feedback, which can be much less effective than utilizing both visual and haptic feedback [27], [28]. Such scenarios are not uncommon in HITL systems, which underscores the importance of safety from instability. These experimental results demonstrate the effectiveness of the rate-limiter as a safety mechanism.

4) Bounded Jerk Perspective: In literature on pHRI with an exoskeleton, it is known that smooth human-like trajectories can be generated by minimizing jerk (time-derivative of acceleration) [29], [30], [31]. Consequently, a trajectory with high jerk appears as unnatural and robotic. Thus, another perspective to the method of this study is that it promotes more natural movements by rate-limiting the human-applied torque signals and thus bounding the jerk of the position trajectories generated by the admittance controller.

VI. Conclusion

In this paper, we show how rate-limiting human-applied torque signals for pHRI on the EXO-UL8 exoskeleton can prevent diverging instability due to time-delay. Specifically, we model the HITL system as: a human as a proportional controller with constant delay, a rate-limiter on the output of the human's applied torques, and a linear second-order virtual dynamics model enabled by admittance control. Our analysis shows that even for large destabilizing time-delays, the trajectories of the HITL system are attracted to a stable limit cycle that can be bound by selecting a sufficiently small rate-limiter threshold. We experimentally validate the rate-limiter through 16 trials corresponding to 4 time-delays and 4 rate-limiter thresholds for each of 10 subjects. Results agree with theory across all time-delays for moderate and large rate-limiter thresholds, and show the limitations of the

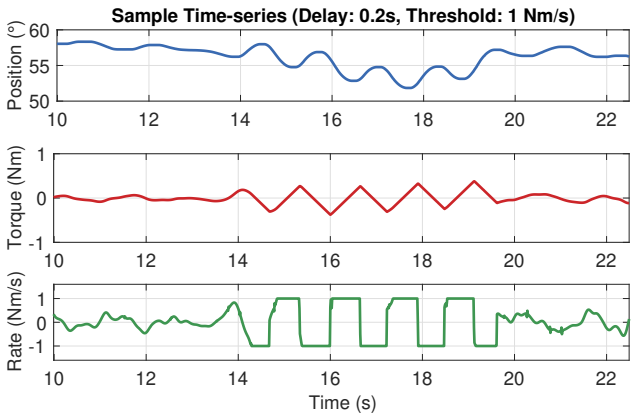

Fig. 9. A time-series showing the rate-limiter suppressing an unstable oscillation and enabling recovery. Oscillations begin to diverge at 14 s due to high time-delay ($d = 0.2$ s), at which point the behavior follows the predicted limit cycle of Fig. 5 until the operator relaxes and regains control at 20 s.

proportional controller human model for very small rate-limiter thresholds. The results demonstrate that the rate-limiter is effective at preventing instability due to large time-delays, and allows the human to recover from delay-induced oscillations, all with minimal interference to regular operation.

REFERENCES

[1] A. Q. Keemink, H. van der Kooij, and A. H. Stienen, "Admittance control for physical human–robot interaction," *The International Journal of Robotics Research*, vol. 37, no. 11, pp. 1421–1444, 2018.

[2] S. F. Atashzar, H.-Y. Huang, F. D. Duca, E. Burdet, and D. Farina, "Energetic Passivity Decoding of Human Hip Joint for Physical Human-Robot Interaction," *IEEE Robot. Autom. Lett.*, vol. 5, no. 4, pp. 5953–5960, 2020.

[3] D. Buongiorno, D. Chiaradia, S. Marcheschi, M. Solazzi, and A. Frisoli, "Multi-DoFs Exoskeleton-Based Bilateral Teleoperation with the Time-Domain Passivity Approach," *Robotica*, vol. 37, no. 9, pp. 1641–1662, 2019.

[4] U. Keller, H. J. A. van Hedel, V. Klamroth-Marganska, and R. Riener, "ChARMin: The First Actuated Exoskeleton Robot for Pediatric Arm Rehabilitation," *IEEE/ASME Trans. Mechatron.*, vol. 21, no. 5, pp. 2201–2213, 2016.

[5] A. M. Khan, D.-w. Yun, M. A. Ali, K. M. Zuhaib, C. Yuan, J. Iqbal, J. Han, K. Shin, and C. Han, "Passivity based adaptive control for upper extremity assist exoskeleton," *Int. J. Control Autom. Syst.*, vol. 14, no. 1, pp. 291–300, 2016.

[6] M. J. Kim, W. Lee, C. Ott, and W. K. Chung, "A passivity-based admittance control design using feedback interconnections," in *2016 IEEE/RSJ International Conference on Intelligent Robots and Systems (IROS)*, pp. 801–807, IEEE, 2016.

[7] F. Just, Ö. Özen, P. Bösch, H. Bobrovsky, V. Klamroth-Marganska, R. Riener, and G. Rauter, "Exoskeleton transparency: Feed-forward compensation vs. disturbance observer," *at - Automatisierungstechnik*, vol. 66, no. 12, pp. 1014–1026, 2018.

[8] D. L. Castro, C.-H. Zhong, F. Braghin, and W.-H. Liao, "Lower Limb Exoskeleton Control via Linear Quadratic Regulator and Disturbance Observer," in *2018 IEEE International Conference on Robotics and Biomimetics (ROBIO)*, pp. 1743–1748, IEEE, 2018.

[9] C. Chen, S. Zhang, X. Zhu, J. Shen, and Z. Xu, "Disturbance Observer-Based Patient-Cooperative Control of a Lower Extremity Rehabilitation Exoskeleton," *Int. J. Precis. Eng. Manuf.*, vol. 21, no. 5, pp. 957–968, 2020.

[10] A. Vick, D. Surdilovic, and J. Kruger, "Safe physical human-robot interaction with industrial dual-arm robots," in *9th International Workshop on Robot Motion and Control*, pp. 264–269, IEEE, 2013.

[11] H. Rifaï, S. Mohammed, W. Hassani, and Y. Amirat, "Nested saturation based control of an actuated knee joint orthosis," *Mechatronics*, vol. 23, no. 8, pp. 1141–1149, 2013.

[12] H.-B. Kang and J.-H. Wang, "Adaptive control of 5 DOF upper-limb exoskeleton robot with improved safety," *ISA Transactions*, vol. 52, no. 6, pp. 844–852, 2013.

[13] F. Dimeas and N. Aspragathos, "Online Stability in Human-Robot Cooperation with Admittance Control," *IEEE Trans. Haptics*, vol. 9, no. 2, pp. 267–278, 2016.

[14] F. Ferraguti, C. Talignani Landi, L. Sabattini, M. Bonfè, C. Fantuzzi, and C. Secchi, "A variable admittance control strategy for stable physical human–robot interaction," *The International Journal of Robotics Research*, vol. 38, no. 6, pp. 747–765, 2019.

[15] H. Kim and W. Yang, "Variable Admittance Control Based on Human–Robot Collaboration Observer Using Frequency Analysis for Sensitive and Safe Interaction," *Sensors*, vol. 21, no. 5, p. 1899, 2021.

[16] T. Zhang, M. Tran, and H. Huang, "Admittance Shaping-Based Assistive Control of SEA-Driven Robotic Hip Exoskeleton," *IEEE/ASME Trans. Mechatron.*, vol. 24, no. 4, pp. 1508–1519, 2019.

[17] O. Baser, H. Kizilhan, and E. Kilic, "Employing variable impedance (stiffness/damping) hybrid actuators on lower limb exoskeleton robots for stable and safe walking trajectory tracking," *Journal of Mechanical Science and Technology*, vol. 34, no. 6, pp. 2597–2607, 2020.

[18] D. H. Klyde, D. T. McRuer, and T. T. Myers, "Pilot-Induced Oscillation Analysis and Prediction with Actuator Rate Limiting," *Journal of Guidance, Control, and Dynamics*, vol. 20, no. 1, pp. 81–89, 1997.

[19] T. Mandal and Y. Gu, "Analysis of Pilot-Induced-Oscillation and Pilot Vehicle System Stability Using UAS Flight Experiments," *Aerospace*, vol. 3, no. 4, p. 42, 2016.

[20] S. L. Gatley, M. C. Turner, I. Postlethwaite, and A. Kumar, "A comparison of rate-limit compensation schemes for pilot-induced-oscillation avoidance," *Aerospace Science and Technology*, vol. 10, no. 1, pp. 37–47, 2006.

[21] J. Yuan, S. Fei, and Y. Chen, "Compensation strategies based on Bode step concept for actuator rate limit effect on first-order plus time-delay systems," *Nonlinear Dyn*, vol. 99, no. 4, pp. 2851–2866, 2020.

[22] X.-h. Liang, K. Yamada, N. Sakamoto, and I. Jikuya, "Model Predictive Controller Design to Suppress Rate-Limiter-Based Pilot-Induced Oscillations," *Trans. Japan Soc. Aero. S Sci.*, vol. 49, no. 166, pp. 239–245, 2007.

[23] J. Sun, Y. Shen, and J. Rosen, "Sensor Reduction, Estimation, and Control of an Upper-Limb Exoskeleton," *IEEE Robot. Autom. Lett.*, vol. 6, no. 2, pp. 1012–1019, 2021.

[24] Y. Shen, J. Sun, J. Ma, and J. Rosen, "Admittance Control Scheme Comparison of EXO-UL8: A Dual-Arm Exoskeleton Robotic System," in *2019 IEEE 16th International Conference on Rehabilitation Robotics (ICORR)*, pp. 611–617, 2019.

[25] E. Cavallaro, J. Rosen, J. Perry, and S. Burns, "Real-Time Myoprocessors for a Neural Controlled Powered Exoskeleton Arm," *IEEE Trans. Biomed. Eng.*, vol. 53, no. 11, pp. 2387–2396, 2006.

[26] P. F. Vint, S. P. Mclean, and G. M. Harron, "Electromechanical delay in isometric actions initiated from nonresting levels," *Medicine and Science in Sports and Exercise*, vol. 33, no. 6, pp. 978–983, 2001.

[27] T. Abuhamdia and J. Rosen, "Constant Visual and Haptic Time Delays in Simulated Bilateral Teleoperation: Quantifying the Human Operator Performance," *Presence: Teleoperators and Virtual Environments*, vol. 22, no. 4, pp. 271–290, 2013.

[28] R. Shadmehr and F. A. Mussa-Ivaldi, "Adaptive representation of dynamics during learning of a motor task," *J. Neurosci.*, vol. 14, no. 5, pp. 3208–3224, 1994.

[29] C. Nguiadem, M. Raison, and S. Achiche, "Motion Planning of Upper-Limb Exoskeleton Robots: A Review," *Applied Sciences*, vol. 10, no. 21, p. 7626, 2020.

[30] L. I. Lugo-Villeda, A. Frisoli, O. Sandoval-Gonzalez, M. A. Padilla, V. Parra-Vega, C. A. Avizzano, E. Ruffaldi, and M. Bergamasco, "Haptic guidance of Light-Exoskeleton for arm-rehabilitation tasks," in *RO-MAN 2009 - The 18th IEEE International Symposium on Robot and Human Interactive Communication*, pp. 903–908, IEEE, 2009.

[31] T. Flash and N. Hogan, "The coordination of arm movements: An experimentally confirmed mathematical model," *J. Neurosci.*, vol. 5, no. 7, pp. 1688–1703, 1985.